

ENSO related variability in the Southern Hemisphere, 1948–2000

Pedro Ribera¹ and Michael E. Mann²

Received 5 July 2002; revised 10 October 2002; accepted 24 October 2002; published 3 January 2003.

[1] The spatiotemporal evolution of Southern Hemisphere climate variability is diagnosed based on the use of the NCEP reanalysis (1948–2000) dataset. Using the MTM-SVD analysis method, significant narrowband variability is isolated from the multi-variate dataset. It is found that the ENSO signal exhibits statistically significant behavior at quasiquadrennial (3–6 yr) timescales for the full time-period. A significant quasibiennial (2–3 yr) timescales emerges only for the latter half of period. Analyses of the spatial evolution of the two reconstructed signals shed additional light on linkages between low and high-latitude Southern Hemisphere climate anomalies. *INDEX TERMS:* 3309 Meteorology and Atmospheric Dynamics: Climatology (1620); 3339 Meteorology and Atmospheric Dynamics: Ocean/atmosphere interactions (0312, 4504); 3349 Meteorology and Atmospheric Dynamics: Polar meteorology. *Citation:* Ribera, P., and M. E. Mann, ENSO related variability in the Southern Hemisphere, 1948–2000, *Geophys. Res. Lett.*, 30(1), 1006, doi:10.1029/2002GL015818, 2003.

1. Introduction

[2] Numerous empirical studies have established the importance of the El Niño/Southern Oscillation (ENSO) on climate variability in the Southern Hemisphere, including both low-latitude regions, such as Australia and South America, and high-latitude regions including Antarctica [Robertson and Mechoso, 1998; Renwick and Revell, 1999; Venegas and Drinkwater, 2001; Venegas et al., 2001; Kidson and Renwick, 2002]. Other potentially distinct modes of climate variability have been argued to influence higher southern latitudes. Such modes include the Antarctic Circumpolar Wave (ACW) and Antarctic Oscillation (AAO) [e.g. Allan et al., 1996; White and Peterson, 1996; Garreaud and Battisti, 1999; Gong and Wang, 1999; Allan, 2000; Carril and Navarra, 2001; Mo and Hakkinen, 2001]. Recent studies suggest that ENSO itself may provide a controlling influence on these latter modes of variability [Carril and Navarra, 2001; Kwok and Comiso, 2002].

[3] Ribera and Mann [2002] simultaneously analyzed four atmospheric variables—temperature, geopotential height, and zonal and meridional wind components—at two different vertical levels (1000 hPa and 500 hPa levels), over the Northern Hemisphere, using NCEP reanalysis data [Kalnay et al., 1996]. They employed the MultiTaper Method-Singular Value Decomposition (MTM-SVD) methodology [Mann and Park, 1999] to isolate spatially-coherent patterns

of narrowband variability that are present in one or more climate fields simultaneously during the latter half of the 20th century. This analysis established ENSO as the only clear source of oscillatory variability in the climate on interannual timescales. We here present a parallel analysis of the Southern Hemisphere. As in Ribera and Mann [2002] this analysis leads us to focus on ENSO, and the atmospheric dynamical linkages between tropical/subtropical and high latitudes expressions of the ENSO signal.

2. Data and Methods

[4] The MTM-SVD technique [Mann and Park, 1999] is applied to the joint surface and mid-tropospheric datasets to isolate statistically significant narrowband, oscillatory patterns of variance that are coherent within and between each of the variables and altitude levels. The MTM-SVD analysis both establishes the timescales of any statistically significant oscillatory signals through a local fractional variance ('LFV') spectrum, and allows for the temporal and spatial reconstruction of the associated signal (see Mann and Park, 1999 for details).

[5] The data used in this study consists of 53 years of monthly anomalies of geopotential height, temperature, zonal and meridional components of the wind, each sampled at two different vertical levels: 1000 hPa and 500 hPa. The selected vertical levels are representative of processes in the low (near surface) and mid troposphere. Simultaneous analysis of the behavior of these atmospheric variables provides the opportunity to follow the dynamical evolution of any climate signals detected. All data fields are taken from the NCEP-NCAR Reanalysis product [Kalnay et al., 1996; White, 2000]. The spatial and temporal scales used in the analysis minimize the error induced by the erroneous introduction of the Australian PAOBS (Australian Surface Pressure Bogus data for the Southern Hemisphere) SLP data south of 40° S [Kistler et al., 2001]. Spurious trends in the data may result from an error in the processing of the Tiros Operational Vertical Sounder (TOVS) data (http://wesley.wvb.noaa.gov/tovs_problem/), and to the presence of some other potential limitations and biases in the data (see Hurrell and Trenberth, 1998 for a detailed discussion)

[6] The data fields are available over a 5° longitude by 5° latitude grid, covering the whole Southern Hemisphere from 0° to 85°S. Prior to analysis, the monthly gridpoint data were converted into standardized anomalies, and then weighted by a gridpoint areal extent factor (cosine of latitude). The expression of the signal at the 500 hPa level was determined through projection of the near-surface (1000 hPa) signal on to the 500 hPa level. This latter step was accomplished through the use of highly reduced (factor of 0.001) gridpoint weighting factors in the analyses for the 500 hPa data. Separate projection analyses were employed

¹Departamento de Ciencias Ambientales, Universidad Pablo de Olavide, Sevilla, Spain.

²Department of Environmental Sciences, University of Virginia, Charlottesville, Virginia, USA.

for each of the four 500 hPa variables (temperature, geopotential height, and wind anomaly components) owing to constraints on the size of the data matrix used in the MTM-SVD signal reconstruction procedure.

3. Analysis

[7] The MTM-SVD analyses employed 3 data tapers and a time-frequency bandwidth product $w = 2N$, providing a frequency resolution equal to half the Rayleigh frequency, and admitting three independent spectral estimates at each frequency [see *Mann and Park, 1999*]. The resulting LfV spectrum for the full 1948–2000 data set (Figure 1) shows a remarkable similarity to a previous analysis of Northern Hemisphere data [*Ribera and Mann, 2002*], as well as broad similarity with previous findings of other researchers [*Barnett, 1991; Mann and Park, 1994; Jiang et al., 1995; Allan et al., 1996; Allan, 2000*], indicating a band of statistically significant quasi-quadrennial ('QQ') variability from 3 to 6 year period (from $f = 0.17$ to $f = 0.33$ cycle-per-year) and a more marginally significant (<90%) band of variance at quasibiennial ('QB') timescales (2–3 yr period). An additional analysis confined to low-latitudes only (0–30° S), yielded an LfV spectrum (not shown) displaying a more prominent QQ signal and, in particular, a considerably more prominent (95% significance) QB signal. Results of this latter analysis are consistent with the presence in the full data of primarily tropical (QQ and QB) signals exhibiting more limited extratropical linkages. As discussed in more detail below, the associated signals are closely associated with ENSO.

[8] In order to investigate the evolution of the frequency and amplitude of the signal, an evolutive LfV spectrum [*Mann and Park, 1996, 1999*] was obtained based on performing the MTM-SVD analysis in a moving 25 year window (Figure 1b). A statistically significant secular variation (corresponding to timescales greater than 12 years in the evolutive analysis) is evident, but this signal is difficult to meaningfully interpret. As described previously, complications related to documented changes in data assimilation could lead to spurious trends in the data [*Hurrell and Trenberth, 1998; Kistler et al., 2001*]. Multiple competing sources of interdecadal variability during the 20th century [e.g., *Mann and Park, 1994; Moron et al., 1998; Allan, 2000; Tourre et al., 2001*], moreover, complicate the interpretation of trends on a decadal timescale. Of interest in this study is the significant interannual variability that is evident. A significant QQ variance peak is centered at frequency $f = 0.30$ cycle/year (3.3 yr period) in the early part of the interval, but appears to split into two distinct bands centered at $f = 0.33$ (3 yr period) and $f = 0.25$ (4 yr period). A significant QB peak centered near $f = 0.45$ (2.2 yr period) emerges in the final decades of the interval. This result is consistent with previous studies arguing for a QB signal of increased amplitude during the past few decades [*Kestin et al., 1998; Allan, 2000*]. The equivalent evolutive MTM-SVD spectra obtained by *Ribera and Mann [2002]* for the Northern Hemisphere exhibit very similar time-frequency patterns of statistically significant variance (for both the full and low-latitude only data) to those obtained in the present study.

[9] Detailed spatial maps of the evolution of the QQ signal are shown (Figure 2) for the most prominent variance

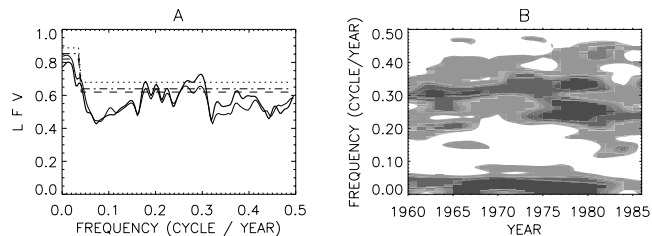


Figure 1. (a) LfV spectrum (1948–2000) for the Southern Hemisphere (thick) and the Northern Hemisphere (light; from *Ribera and Mann, 2002*) with 90%, 95% and 99% significance levels. (b) Evolutive spectrum with a 25 yr window. Significance is indicated by grayshading, color scale indicates 50% confidence level (light grey), 90%, 95% and 99% (black).

peak evident in the evolutive LfV spectrum (Figure 1b—the peak near $f = 0.3$ cycle/yr that is pronounced during the first half of the data interval). As in *Ribera and Mann [2002]*, the signal reconstruction follows the evolution of the signal through one half cycle in quarter-cycle (45 degree) phase increments, from peak warm ENSO event conditions (i.e., maximum air temperature anomaly at 1000 hPa at 100° W over the Equator), defined as ‘zero phase’, to peak cold ENSO event (‘180 degree phase’) conditions. Anomalies at 180 degrees phase are, by construction, opposite to those observed at 0 degrees phase. A three dimensional continuous animation of the signal evolution can be obtained on the internet: <http://holocene.evsc.virginia.edu/supplement/pribera>. The spatial patterns associated with the other interannual variance peaks noted in Figure 1 show a similar ENSO-type pattern. In each case, surface warming in the eastern and central equatorial Pacific is accompanied by negative anomalies in overlying geopotential heights. Positive surface geopotential height anomalies over the Pacific Australian coast during the warm phase of ENSO are consistent with an inhibition of convection, and thus, the typical association of El Niño with drought in the region.

[10] Among the more distantly teleconnected anomalies, of particular interest is the apparent connection between the low-latitude ENSO signal and geopotential height and surface temperature anomalies in the high-latitude, Antarctic region. Neighboring centers of positive and negative near-surface geopotential height anomalies over Antarctica are observed to evolve in amplitude and sign through the QQ cycle (Figure 2). This structure is very similar to the wave number 2 pattern in the circumpolar Southern Ocean that *Kwok and Comiso [2002]* correlate with the Southern Oscillation Index (SOI). The signal reconstruction shown in Figure 2 (see the on-line animation for more details) suggests a particular dynamical evolution by which the QQ signal propagates from the eastern tropical Pacific SST anomalies to the Antarctica. The equatorial surface signal appears to modulate the upper level geopotential field north of Antarctica, which appears to then propagate down through the troposphere leading to a nearly equivalent barotropic structure of pressure anomalies, and a resulting pattern of near-surface temperature anomalies over Antarctica that is consistent with the anomalous surface circulation. Changes in the position of the high-latitude geopotential height anomaly appear to follow changes in

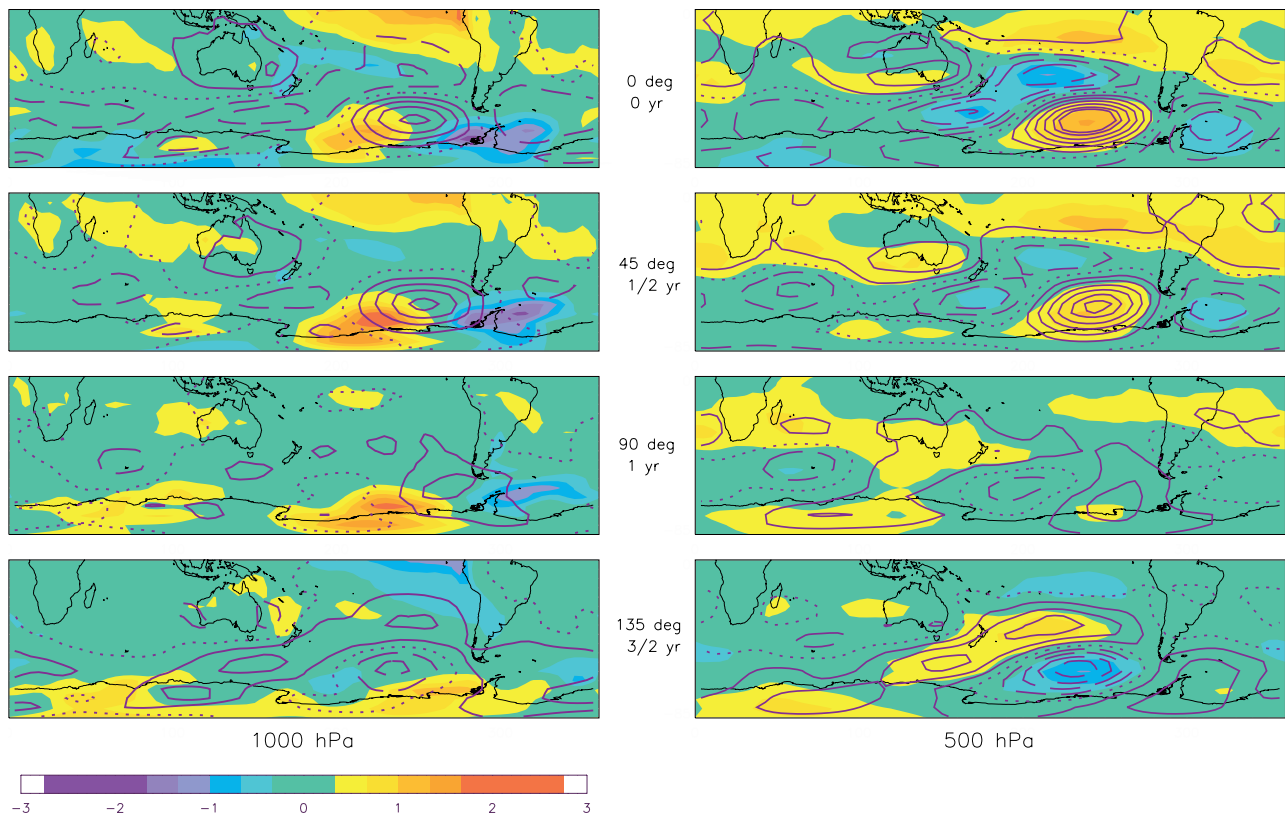


Figure 2. Spatial reconstructions of QQ oscillation (Phases 0° , 45° , 90° and 135°). Temperature anomalies are indicated by the associated color scale. Geopotential height anomalies are indicated by (magenta) contours (solid line: positive anomalies, dashed line: negative anomalies, dotted line: zero contour, intervals shown indicate \dots , -16 , -8 , 0 , 8 , 16 , \dots m anomalies).

the position of the tropical heating, and the transition in the sign of the upper-level geopotential height anomaly appears to coincide with the transition from the warm to cold-event phase. The associated evolution of the surface temperature field resembles quite closely, in places, the ‘Antarctic Circumpolar Wave’ (ACW), but, in our interpretation is associated simply with an evolving pattern of near-surface temperature advection that follows changing near-surface geopotential anomalies.

[11] The correlation between the QQ ENSO signal reconstruction and the AAO series (1958–1999) shows the two to be significantly (negatively) correlated at roughly 90 degrees out of phase. Peak negative AAO conditions coincide roughly with the 90° phase pattern (Figure 2) of the QQ ENSO signal. This finding is not inconsistent with previous work [Schneider and Steig, 2002] arguing for minimal *contemporaneous* (i.e., zero-lag) correlation between the AAO and ENSO, because the two signals are only highly correlated at a quarter-cycle phase lag. Our findings thus argue for a dynamical relationship, albeit a lagged one, between the AAO and the QQ ENSO signal, and seem to confirm the relationship between ENSO and Antarctic climate anomalies described by Kwok and Comiso [2002] and Schneider and Steig [2002]. Our findings, moreover, confirm the development of anticyclonic circulation and more frequent blocking episodes in the eastern south Pacific during ENSO warm events, as described in Renwick and Revell [1999]; and Kidson and Renwick [2002].

[12] The dipolar structure observed over the Antarctic ocean, and over the eastern and western coasts of South America, is consistent with a air mass displacement through the evolution of the cycle. During the warm phase, a positive surface height anomaly is observed in the Pacific to the north of the Amudsen Sea and a negative height anomaly in the South Atlantic, to the north-east of the Weddell Sea. As a consequence, warm air advection is favored over the area between the Ross and the Amudsen Seas, while cold air is advected over the Weddell Sea, leading to the melting/freezing of sea-ice over the respective areas. This relationship is consistent with the existence of a connection between the ENSO cycle and the production/destruction of Antarctic ice, as noted in other recent studies [Venegas and Drinkwater, 2001; Venegas et al., 2001; Kwok and Comiso, 2002].

[13] Significant differences are evident in our analysis with regard to the apparent nature of extratropical teleconnections of ENSO in the two hemispheres. The evolution of the quasiquadrennial (QQ) signal in the Northern Hemisphere [Ribera and Mann, 2002] indicates a pattern of mass transport over the course of the cycle that is largely confined to the Pacific basin. In contrast, the QQ signal in the Southern Hemisphere suggests mass transport between the Indian, Pacific and Atlantic basins. The associated patterns of heat and mass transport suggest a direct influence of ENSO on the equatorial Pacific and Indian oceans, and an extratropical influence on the South Atlantic ocean.

4. Conclusions

[14] The only clear oscillatory interannual signal in tropospheric climate during the later half of the 20th century in the Southern Hemisphere is associated with the ENSO phenomenon, characterized by a 'quasi-quadrennial' band of variance centered at 3–6 year period and a weaker and more intermittent 'quasi-biennial' band of variance centered at 2–3 year period. The spatial evolution of the ENSO signal, as characterized in multiple fields of the NCEP reanalysis data, synthesizes a number of previous distinct observations regarding low-to-high latitude ENSO linkages in the Southern Hemisphere. Particularly interesting is the direct connection between low-latitude surface temperature anomalies and the Antarctic Circumpolar Wave and Antarctic Oscillation patterns of the high-latitude Southern Ocean and Antarctic periphery.

References

- Allan, R. J., J. A. Lindesay, and D. E. Parker, El Niño Southern Oscillation and Climatic Variability, CSIRO Publications, Melbourne, Australia, 405 pp., 1996.
- Allan, R. J., ENSO and climatic variability in the last 150 years, edited by H. F. Diaz and V. Markgraff, in Chapter 1, El Niño and the Southern Oscillation: Multiscale variability, Global and Regional Impacts, Cambridge University Press, Cambridge, UK, 3–56, 2000.
- Barnett, T. P., The Interaction of Multiple Time Scales in the Tropical Climate System, *J. Climate*, 4, 269–285, 1991.
- Carril, A. F., and A. Navarra, Low-Frequency Variability of the Antarctic Circumpolar Wave, *Geophysical Research Letters*, 28, 4623–4626, 2001.
- Garreaud, A. D., and D. S. Battisti, Interannual (ENSO) and interdecadal (ENSO-like) variability in the Southern Hemisphere tropospheric circulation, *J. Climate*, 12, 2113–2123, 1999.
- Gong, D. Y., and S. W. Wang, Definition of Antarctic Oscillation Index, *Geophysical Research Letters*, 26, 459–462, 1999.
- Hurrell, J. W., and K. E. Trenberth, Difficulties in Obtaining Reliable Temperature Trends: Reconciling the Surface and Satellite Microwave Sounding Unit Records, *J. Climate*, 11, 945–967, 1998.
- Jiang, N., J. D. Neelin, and M. Ghil, Quasi-quadrennial and quasi-biennial variability in the equatorial Pacific, *Clim. Dyn.*, 12, 101–112, 1995.
- Kalnay, E., et al., The NCEP/NCAR 40-year reanalysis project, *Bull. Amer. Meteor. Soc.*, 77, 437–471, 1996.
- Kestin, T. S., D. J. Karoly, J. Yano, and N. A. Rayner, Time-frequency variability of ENSO and stochastic simulations, *J. Climate*, 11, 2258–2272, 1998.
- Kidson, J. W., and J. A. Renwick, The Southern Hemisphere Evolution of ENSO during 1981–1999, *J. Climate*, 15, 847–863, 2002.
- Kistler, et al., The Ncep-Near 50-Year Reanalysis: Monthly Means Cd-Rom and Documentation, *Bull. Amer. Meteor. Soc.*, 82, 247–267, 2001.
- Kwok, R., and J. C. Comiso, Southern Ocean Climate and Sea Ice Anomalies Associated With the Southern Oscillation, *J. Climate*, 15, 487–501, 2002.
- Mann, M. E., and J. Park, Global-scale modes of surface temperature variability on interannual to century timescales, *J. Geophys. Res.*, 99(D12), 1994.
- Mann, M. E., and J. Park, Joint Spatio-Temporal Modes of Surface Temperature and Sea Level Pressure Variability in the Northern Hemisphere During the Last Century, *J. Climate*, 9, 2137–2162, 1996.
- Mann, M. E., and J. Park, Oscillatory Spatiotemporal Signal Detection in Climate Studies: A Multiple-Taper Spectral Domain Approach, *Advances in Geophysics*, 41, 1–131, 1999.
- Mo, K. C., and S. Hakkinen, Interannual Variability in the Tropical Atlantic and Linkages to the Pacific, *J. Climate*, 14, 2740–2761, 2001.
- Moron, V., R. Vautard, and M. Ghil, Trends, interdecadal and interannual oscillations in global sea-surface temperature, *Clim. Dyn.*, 14, 545–569, 1998.
- Renwick, J. A., and M. J. Revell, Blocking over the South Pacific and Rossby Wave Propagation, *Mon. Wea. Rev.*, 127, 2233–2247, 1999.
- Ribera, P., and M. E. Mann, Interannual variability in the NCEP Reanalysis 1948–1999, *Geophysical Research Letters*, 29, 132-1–132-4, 2002.
- Robertson, A. W., and C. R. Mechoso, Interannual and Decadal Cycles in River Flows of Southern South America, *J. Climate*, 11, 2570–2581, 1998.
- Schneider, D. P., and E. J. Steig, Spatial and temporal variability of Antarctic ice sheet microwave brightness temperatures, *Geophysical Research Letters*, 10.1029/2002GL015490, 2002.
- Tourre, Y. M., R. Rajagopalan, Y. Kushnir, M. Barlow, and W. B. White, Patterns of Coherent Decadal and Interdecadal Climate Signals in the Pacific Basin during the 20th Century, *Geophysical Research Letters*, 28, 2069–2072, 2001.
- Venegas, S. A., and M. R. Drinkwater, Sea Ice, Atmosphere and Upper Ocean Variability in the Weddell Sea, Antarctica, *Journal of Geophysical Research - Oceans*, 106, 16,747–16,766, 2001.
- Venegas, S. A., M. R. Drinkwater, and G. Shaffer, Coupled Oscillations in Antarctic Sea Ice and Atmosphere in the South Pacific Sector, *Geophysical Research Letters*, 28, 3301–3304, 2001.
- White, G. H., Long-term trends in the NCEP/NCAR reanalysis, Proceedings of the Second WCRP International Conference on Reanalysis, pp. 54–57, 2000.
- White, W. B., and R. G. Peterson, An Antarctic Circumpolar Wave in surface pressure, wind, temperature and sea-ice extent, *Nature*, 380, 699–702, 1996.

P. Ribera, Depto. CC. Ambientales, Univ. Pablo de Olavide, Carretera de Utrera, km 1, Sevilla 41013, Spain. (pribrod@dex.upo.es)

M. E. Mann, Department Environmental Sciences, Clark Hall. Univ. Virginia, Charlottesville, VA 22903, USA. (mann@virginia.edu)